Misan Journal of Engineering Sciences ISSN-E: 2957-4250
Vol. 5, No. 1, 28 June 2026 ISSN: 2957-4242

Effect of Nano-Zirconia Dip Coating on the Surface Properties of PEEK for Dental Implants

Baydaa K.Rahi*[1], Jumaa S. Chiad[2] and Intisar J.Ismail[3]

[1] Department of Biomedical Engineering, College of Engineering, AL-Nahrain University, Baghdad, Iraq
[2]Al-Karkh University of Science, Baghdad, Iraq
[3]Al-Esraa University College of Dentistry, Baghdad, Iraq
Corresponding author E-mail: *Email: bayadaa.mbe23@ced.nahrainuniv.edu.iq

(Received 31 Oct 2025, Revised 4 Feb 2026, Accepted 7 Feb 2026)

Abstract: Dental implants that are biofunctionally coated are placed in a strategic location in bone where they assume an integral function in augmenting the process of healing and promoting bone growth in the implantation site. The purpose of this present study was to evaluate the impact of two different nano-zirconia (ZrO_2) coating thicknesses on dip-coated polyetheretherketone (PEEK) implants by using zirconia nanoparticles with a particle size of 40–50 nm and coating layer thicknesses ranging from 18.25–35.14 µm and 58.67–65.34 µm. Both an uncoated control group of PEEK discs and two groups of PEEK discs coated with varying thicknesses were considered. Surface roughness was determined using a profilometer, and field-emission scanning electron microscopy (FE-SEM) was used to study coating morphology, nanoparticle distribution, and coating thickness by image analysis. X-ray diffraction (XRD) was used to identify crystalline phases of the coating. Water contact angle measurements were also performed to analyze wettability; the thickest coating had a contact angle of 34.17°, indicating a significant increase in hydrophilicity. Adhesion tests indicated good interfacial adhesion for the thinner coating (5B, ASTM D3359). The thicker layer received a slightly lower rating (4B) due to some coating removal along the cut edges. A decrease in adhesion strength with increasing thickness was attributed to the accumulation of internal residual stresses and decreased interfacial cohesion. Overall, nano-ZrO_2 dip coatings improved surface morphology and interfacial performance, suggesting their potential as a reliable surface modification strategy for dental implants.

Keywords: Dip coating, Nano zirconia, Water contact Angle, Adhesion test, XRD

1. Introduction

Missing natural teeth due to tooth decay, periodontal disease, or injury can impair oral functions such as mastication, speech, and facial aesthetics. The increasing demand for dental implants has led to the development of numerous surgical and prosthodontic procedures, thereby driving rapid market expansion [1].PEEK, as a high-performance engineering thermoplastic, is increasingly being used in orthopedic and dental applications for bone reconstruction. Relative to autologous bone, metal, or ceramic implant materials, PEEK has an elastic modulus similar to that of human cortical bone, with a consistent value of 3–4 GPa as well as good biocompatibility, chemical resistance, and thermal stability[2, 3].is currently viewed as an alternative to traditional metallic implants in orthopedic applications due to its enhanced mechanical properties, reduced immunotoxicity, and favorable processing characteristics.. It can also mitigate certain drawbacks associated with metal implants, including stress shielding and metal hypersensitivity[4]. The bioinert property of PEEK may limit its potential therapeutic applications due to

DOI: https://doi.org/10.61263/mjes.v5i1.221
This work is licensed under a Creative Commons Attribution 4.0 International License

a lack of direct osseointegration with surrounding tissues [3]. Enhancements are necessary due to these drawbacks, as a lack of biological reactivity impairs the amount of new host bone formed in vivo. To improve the osseointegration ability of PEEK implants, several surface modification methods, including wet chemical treatment, plasma modification, and electron beam deposition, have been proposed to address this issue [5]. These methods aim to provide surfaces that are porous, hydrophilic ,and textured, which are considered advantageous for dental purposes [6]. Osseointegration, described as the direct structural and functional connection between healthy bone and the surface of a load-bearing implant, is influenced by appropriate implant surface properties[7]. The responses of osteoblasts, which play a crucial role in bone formation, vary with implant materials, depending on their surface geometry and chemistry [8]. Hence, surface modification of PEEK is necessary to enhance the clinical efficacy of this implant[9]. Manipulation of materials at the nanoscale (1–100 nm), or nanotechnology, presents new opportunities in dentistry and has extended to another field, dubbed nanodentistry [10]. The use of nanotechnology has led to significant advances in dental materials, devices, and treatment modalities, such as dental implants [11]. Nanomaterials, particularly high-purity zirconia (ZrO_2), have become among the most promising materials in dentistry due to their superior whiteness and unique physical and chemical properties, including high toughness, mechanical strength, and excellent corrosion resistance [12, 13] .The hardness of bulk ZrO_2 poses manufacturing challenges. However, recent developments in the field suggest that micro- and nanoscale zirconia powders could address this limitation. Nano-ZrO_2 has been used in powder filling or as a surface coating, and as precursors for sintering [14, 15] .Several studies have demonstrated that the incorporation of nano-ZrO_2 significantly improves the flexural strength, fracture toughness, and adhesion strength of dental ceramics and scaffolds. Furthermore, nano-ZrO_2 is a highly promising porous surface-coating material. Its nanoscale characteristics enhance the biocompatibility and osseointegration of dental implants .To obtain a uniform nano-ZrO_2 layer on the surface of the PEEK specimens, the deposition process was performed via dip coating, the most common method for deposition at both industrial and laboratory levels. This may be attributed to the efficiency, cost-effectiveness, and superior quality of coating[15]. The process involves immersing the substrates in the coating solution and then withdrawing them from the solution[16]. Dip coating is ideally suited for coating relatively flat or rod-shaped rigid substrates; however, modified techniques can be used to coat substrates with more complex geometry. Generally, the substrate material must be resistant to the coating liquid and heat. Moreover, the substrate should be impermeable to prevent the liquid coating from penetrating it. The coating material is dried to achieve the desired film thickness. While drying is typically carried out at room temperature or at temperatures as high as 250°C, this is not always the case [15]. As a result, two different coating thicknesses were used to study the effect of thickness variation on surface properties. The study seeks to investigate whether any correlation exists between coating thickness and variations in surface morphology, wettability, and adhesion strength, thereby enabling researchers to determine the optimal thickness that yields the most effective surface response and interfacial interactions with the implant. Thus, coating thickness is one of the important factors that contribute to enhancing the clinical performance of dental implants.

2. Materials and Methods

2.1. Specimen

Medical implant-grade PEEK rods 30 mm in diameter,500 mm in length, and a nominal density of 1.3g/cm^3 (Dongguan Redspot Technology Co., Ltd., China) were selected as substrates. The rods were machined into disk samples having a 30 mm diameter and a 2 mm thickness by a lathe. To prevent the accumulation of fine particles formed during prolonged milling, samples were ultrasonically cleaned in ethanol for 10 min, followed by a 5 min rinse in deionized water to remove any remaining surface debris or impurities. The substrates were then air-dried at ambient temperature and relative humidity without forced ventilation or heating, allowing gradual evaporation of moisture while preserving the integrity of the sample surface. ZrO_2 nanopowder supplied by Hongwu International Group Co., Ltd (99.9% purity, 40–50 nm particle size) was utilized in its original form without further processing. All reaction mixtures were prepared with deionized water.

2.2 Surface Modification

The adhesion of the material to the surface can be improved by modifying the surface characteristics of samples. As a result, PEEK disc samples were initially etched in 98% sulfuric acid for 3 minutes to modify the surface. The subsequent step involved washing the disc with deionized water for 5 minutes. The next step comprised washing the samples in acetone ultrasonically for 10 minutes, followed by three additional ultrasonic washes in deionized water for 5 minutes each, and drying at 37°C. This process was conducted to increase surface roughness prior to coating, given that PEEK has a naturally low surface roughness, thereby reducing the surface area available for the coating to adhere. A previous study has provided a more detailed explanation of this procedure [17, 18].

2.3 Coating Procedure

Coating is a process of one material applied to another, irrespective of their purpose, which can even be used for surface modification. This part of the study involved preparing a dip-coating solution by dissolving 2 g of polyvinylpyrrolidone (PVP, K30; India) in 30 mL of distilled water using a magnetic stirrer (ALFA-HS860; Iran). After that, 6 g of zirconia nanopowder (ZrO_2, 40–50 nm, Hongwu International Group Ltd., China) was added and homogenized for 20 minutes. The complete volume was then adjusted by adding 70 mL of absolute ethanol (99%, CDH, India), and the mixture was stirred further to obtain a homogeneous, stable coating solution. Polyetheretherketone (PEEK) samples pretreated with concentrated sulfuric acid were immersed vertically in the resulting solution for 20 s and then removed. They were left to air-dry for 5 min to form a first layer of coating. The dip–drying cycle was repeated 3 times for the low-thickness group and 6 times for the high-thickness group to obtain two different coating thicknesses. Finally, after coating, all the samples were heat-treated in a drying oven at 100 °C for one h under atmospheric air to enhance layer adhesion and stability[19, 20].

2.4 Coating Analysis

The coated layers were characterized to evaluate the surface morphology and structural features of the treated samples. The surface morphology of the coated samples was studied using FE-SEM. The roughness (Ra, µm) of the samples was quantitatively evaluated using a contact stylus profiler (TR200, TIME Group, Germany). Three readings on the center of each disc sample were obtained along parallel lines with a traversal distance of 5.0 mm and a cutoff length of 0.8 mm, and an average was calculated to determine the overall surface properties. The Ra value indicates the mean surface roughness of each sample surface, as determined by profilometer measurements; smaller Ra values indicate smoother surfaces. The phase structure of the samples was tested by X-ray diffraction (XRD). The spectra were obtained using a Cu Kα source (40 kV, 30 mA) over the 10°–80° (2θ) range, with a scanning speed of 10°/min and a step size of 0.04°, on a Shimadzu LabX XRD-6000 diffractometer (Japan). The wetting behavior and relative hydrophilic or hydrophobic nature of coated and non-treated PEEK disks were confirmed by contact angle measurements. The cross-hatch adhesion test was used to determine the adhesiveness of the coatings. Applying pressure was necessary for this process because the coating exhibited strong adhesion to the substrate. Hence, this evaluation represented the adhesion between the coating and the substrate. The process was performed in accordance with ASTM D3359, which specifies the standard method for determining the adhesion of thin, bonded, polymeric coatings. A cutter was then used to create a cross-hatch design on the coated surface; adhesive tape was pressed onto it to achieve the required adhesion strength. After removing the adhesive tape, the surface was examined for any remaining coating on each panel[21, 22].

3. Results and Discussion

3.1 Structure Analysis

FE-SEM was used to examine the surface morphology of the specimens and measure the coating thickness from cross-sectional images. The findings revealed continuous coatings with variations in thickness and layer uniformity. The thickness of the coating layer ranged from 18.25–35.14 µm and 58.67–65.34 µm, as shown in Fig. 1. The variation in thickness was dependent on the number of deposited layers. With each dip-coating cycle, zirconia nanoparticles gradually accumulated, increasing coating thickness and forming denser, more compact multilayered structures.

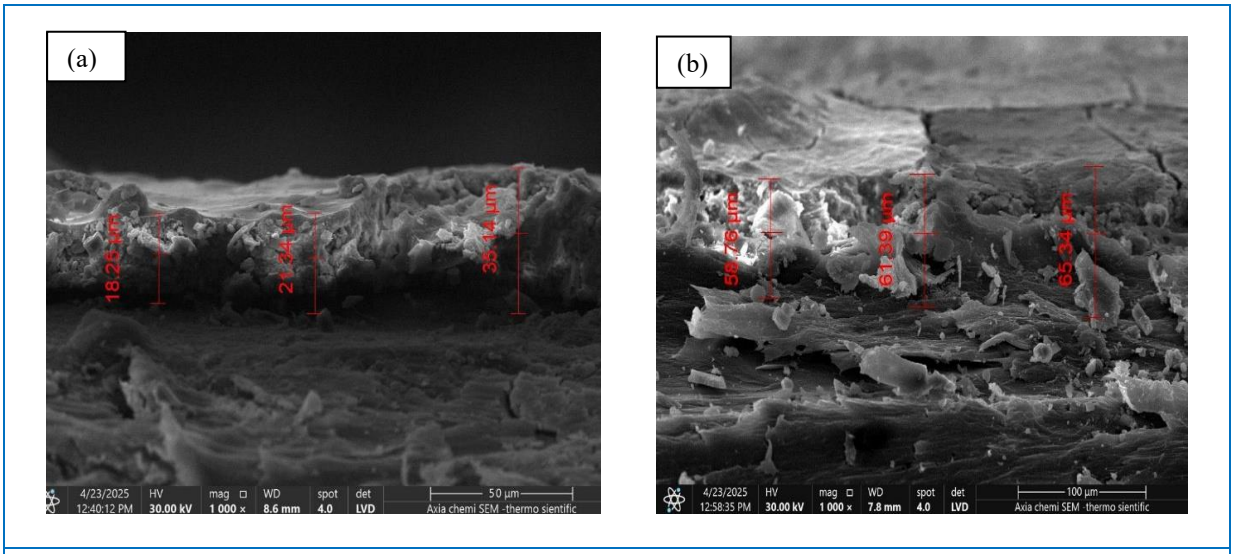


Fig. 1. Coating thickness for (a) sample with low thickness, (b) sample with high thickness

3.2 Field-Emission Scanning Electron Microscopy (FE-SEM) Analysis

Uncoated PEEK samples exhibited parallel milling grooves with no topography. After concentrated H_2SO_4 treatment, nanoscale etched structures were observed, indicating increased surface roughness and successful surface activation. This might be attributed to the interaction between the aromatic group in the PEEK structure and sulfonic groups ($-SO_3H$) generated by sulfuric acid[23]. Nano-ZrO_2-coated specimens exhibited irregular surface morphology, rough surfaces, and varying surface coverage, depending on the coating thickness. The lower-thickness coating exhibited less densely packed nanoparticles, with visible interparticle voids. In contrast, the higher-thickness coating exhibited a denser and more continuous nanoparticle layer with reduced interparticle voids and a more compact surface structure, as shown in Fig. 2. The results demonstrated that coating thickness played an important role in the structural and morphological characteristics of the ZrO_2 layers on PEEK substrates.

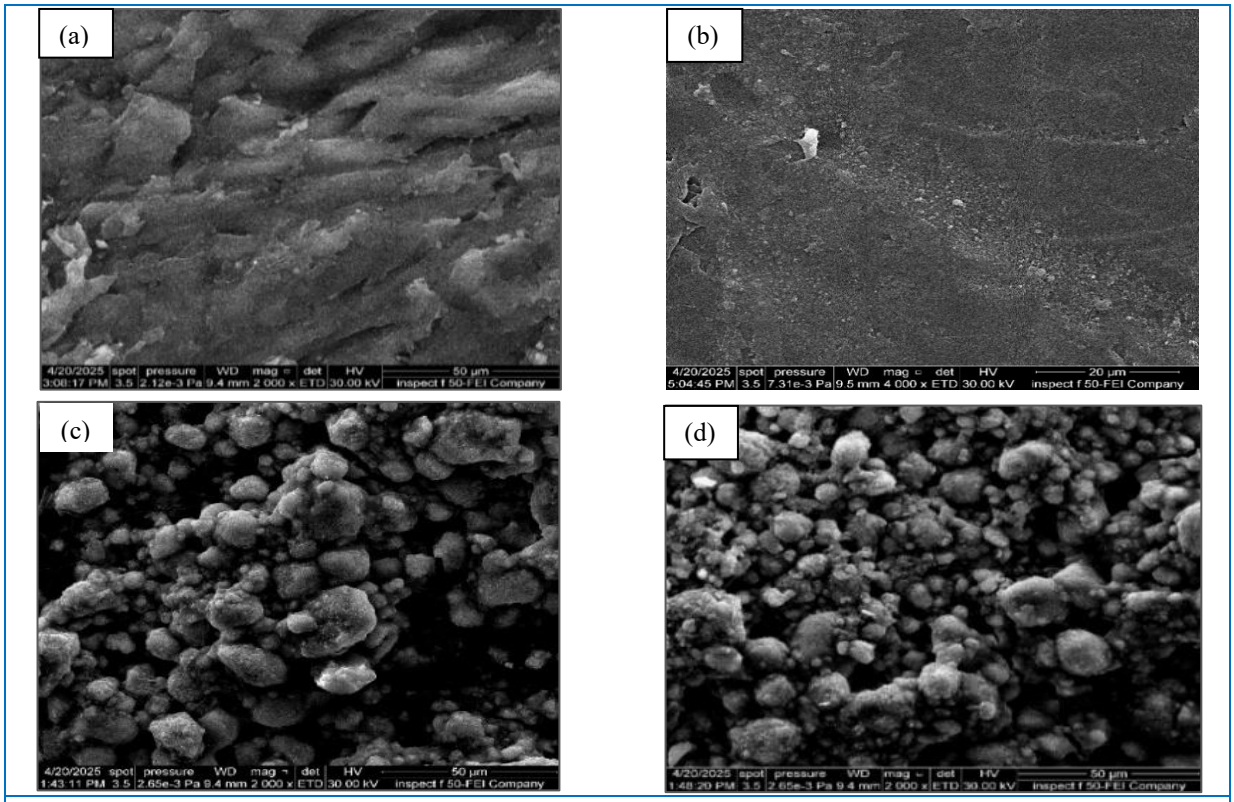


Fig. 2. FESEM images: (a) Control Group, (b) Surface Modified with H_2SO_4,(c) low-Thickness ZrO_2 coating, (d) high-Thickness ZrO_2 coating

3.3 Cross-cut Adhesion Analysis

A cross-cut adhesion test was conducted to evaluate coating delamination from the substrate by incising the coating with a rectangular grid pattern down to the substrate. This method is commonly referred to as pass/fail screening of adhesion. The method can also be used to evaluate the resistance of individual layers to separation in multilayer coating systems. The method followed ASTM D3359 [21]. This provides a six-step classification system Fig.3. For routine purposes, the first three classifications are considered sufficient; however, exceptional circumstances may require the application of the complete six-step scale. The sample with the lower coating achieved 5B without any visible peeling, indicating sound interfacial adhesion between the coating and the PEEK substrate. However, the higher thickness of the coating received a 4B rating because of slight peeling along the cut edges [21, 24]. The enhanced performance was attributed to the incorporation of ZrO_2 nanoparticles into the PVP matrix, leading to strong adhesion to the substrate through mechanical interlocking and chemical bonding. The treatment of the PEEK substrate's complex surface structure benefits from integration with nanoparticles. According to the literature, incorporation of 0.1 wt. % PVP to the composite coating systems remarkably increases the adhesion strength, attributed to realizing better structure uniformity and interfacial interaction between the dispersed nanoparticles and polymer matrix[25, 26].



CLASSIFICATION OF ADHESION TEST RESULTS

CLASSIFICATION	PERCENT AREA REMOVED	SURFACE OF CROSS-CUT AREA FROM WHICH FLAKING HAS OCCURRED FOR SIX PARALLEL CUTS AND ADHESION RANGE BY PERCENT
5B	0% None	
4B	Less than 5%	
3B	5 – 15%	
2B	15 – 35%	
1B	35 – 65%	
0B	Greater than 65%	

Fig. 3. (a) Adhesion cross-hatch test kit and (b) cross-cut guidance[27]

3.4 Wettability Test Analysis

The wettability of PEEK substrate surfaces treated with the appropriate experimental groups was carefully examined by measuring the water contact angles. The control group presented hydrophobicity with a contact angle of 85.159°. In the (18.26–35.14) µm thickness group, a lower contact angle (41.176°) was reported, and better surface hydrophilicity than in the control group was observed. Moreover, the contact angle of the group with coating thickness (58.76–65.34) µm declined to 34.170°, suggesting a significant augmentation in surface wettability at higher coating thickness, as shown in Table 1. The phenomenon of surface wetting is associated with complex behavior at the solid–air and solid–liquid interface. The formation of a solid–liquid interface that releases energy is an exoergic process, whereas generating a liquid–air interface requires the absorption of energy, which is endoergic[28] .The morphology and adhesiveness of water droplets on a substrate are determined by the excess free energy difference between adhesion to the substrate and the cohesive force. The energy released by the connection, but dissipated during wetting of the surface, increases directly with the total wetted area of a roughened surface and exceeds the surface's geometric area. This means that the coating's wettability is strongly influenced by surface roughness. The Wenzel and Cassie-Baxter theories are useful for understanding the effect of surface roughness on water contact angle [29]. In the Wenzel model, wetting on the substrate indentation of a textured surface is examined, and the Cassie-Baxter method gives insight into similar dynamic interactions between water and surface elevations. This model is based on the roughness factor, which measures the extent to which the actual surface is higher than the geometric one. The relationship between contact angle and coating thickness on hydrophilic surfaces is complex and influenced by multiple factors, including surface energy, roughness, and shape. The influence of film thickness on the contact angle of hydrophilic surfaces is presented schematically in Fig. 4[30]. Hydrophilic surfaces are characterized by high surface energy, which enables them to interact strongly with water and other polar liquids. A higher coating thickness also ensures that surface wetting is both more uniform and complete, resulting in a smaller contact angle [31]. The relationship between contact angles and molecular thickness can be theoretically established on hydrophilic substrates [31].

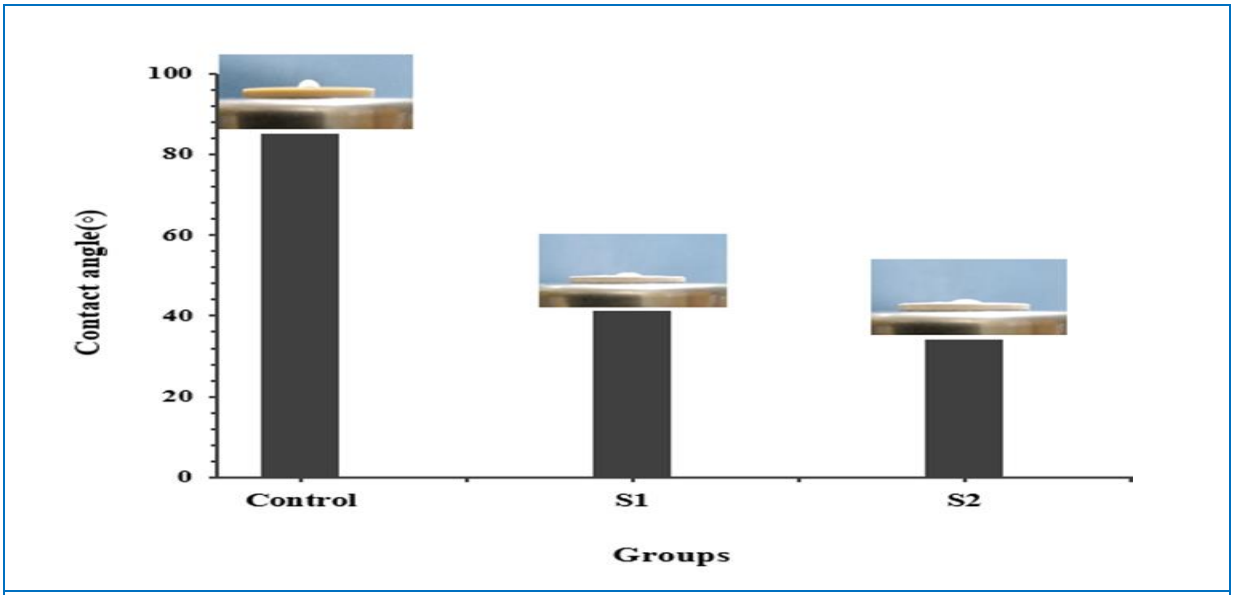


Fig. 4. Comparison of contact angle measurement for control and coated samples. Inset images represent water droplet profiles on each surface

Table 1. Average contact angle of control and coated samples

sample	N. of sample	Average contact angle
control	3	85.159
S1	3	41.167
S2	3	34.170

3.5 Roughness Measurement Analysis

Figure 5 illustrates the quantitative assessment of surface roughness (Ra) values of the control specimens, sulfuric acid-treated specimens, and nano-ZrO_2–coated PEEK specimens with different coating thicknesses. The results indicate that the group of greater thickness recorded the highest surface roughness of 1.965 µm, while the group of lower thickness recorded 1.512 µm. In contrast, sulfuric acid–treated specimens provided a moderate increase value of 0.927 µm compared to untreated control group which recorded 0.637 µm. These findings demonstrate the significant influence of coating thickness on surface roughness, indicating a thickness-dependent surface modification effect. Despite significant developments in biomaterials, determining the ideal surface roughness for optimal osseointegration remains challenging [32]. Thus, optimizing the coating thickness could be an important parameter for enhancing the interfacial response and osseointegration potential of PEEK dental implants.

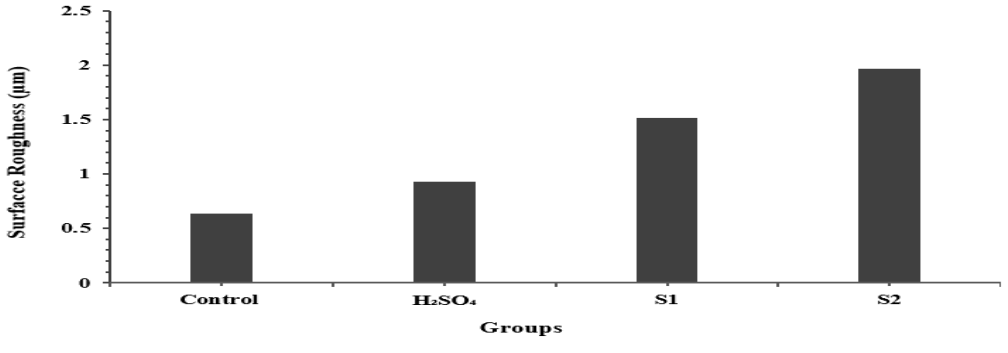


Fig. 5. Average surface roughness (Ra) values of PEEK specimens: control, H_2SO_4-treated, and nano-ZrO_2-coated groups (S1: low thickness, S2: high thickness)

3.6 X-Ray Diffraction (XRD) Analysis

The X-ray diffraction (XRD) pattern in Fig. 6 of the sample coated with a ZrO_2 layer on the PEEK substrate exhibited sharp, well-defined peaks distributed over the 2θ range of 10° to 80°. Distinctive peaks of semicrystalline PEEK were observed at 2θ = 18.62° and 22.06°, which were attributed to the (110) and (220) planes, and agree with previously reported results [33], indicating that the X-rays penetrated the coating layer and reached the underlying polymeric substrate. For the ceramic coating, the strongest reflections at 2θ = 27.59°, 30.89°, and 33.67° were indexed to the (−111), (111), and (020) planes of the monoclinic zirconia (m-ZrO_2) phase, as per JCPDS card No. 03-065-2357. Additional peaks appeared at 40.70°, 49.35°, 54.82°, 59.02°, and 63.68°, corresponding to other crystallographic planes of ZrO_2, which reflects the polycrystalline nature of the deposited layer.

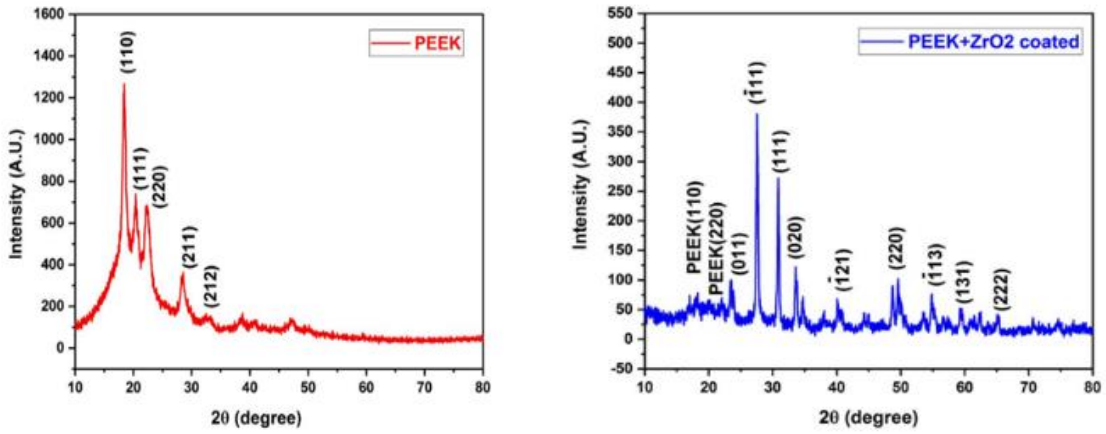


Fig. 6. X-ray diffraction patterns of the(a) uncoated and (b) nano-ZrO_2-Coated PEEK samples

4 Conclusions

The present study demonstrated that dip-coated nano-ZrO_2 coating on PEEK enhanced the coating's surface features and produced a high-quality coating interface. Roughness, wettability, and morphology were all directly affected by the coating thickness. The contact angle measurement confirmed that the hydrophilic nature was improved. In the adhesion test performed in accordance with ASTM D3359, excellent adhesion was demonstrated, and a 5B rating was obtained from the cross-cut adhesion test on the low-thickness coating. With a greater thickness, a slightly lower grade 4B was obtained. XRD analysis confirmed the presence of crystalline zirconia and revealed the preservation of the PEEK structure. Hence, the nano-ZrO_2 coatings used in PEEK dental implants offer a suitable surface modification technique that can improve clinical outcomes and long-term performance. Further work will include evaluating mechanical properties, such as hardness, and testing biocompatibility and antibacterial activity against Gram-positive and Gram-negative bacteria to better define its applicability to dental implants.

Author Contributions: The authors contributed to all parts of the current study.
Funding: This study received no external funding.
Conflicts of Interest: The authors declare no conflict of interest.

References

[1] S. A. Alwan and T. I. Hamad, "Electrospray coating of poly ether ether ketone (PEEK) dental implant material with Zein-CaSiO3 composite," *Journal of Thermoplastic Composite Materials,* vol. 38, no. 3, pp. 893-910, 2025.

[2] K. Lavanya, S. V. Chandran, K. Balagangadharan, and N. Selvamurugan, "Temperature-and pH-responsive chitosan-based injectable hydrogels for bone tissue engineering," *Materials Science and Engineering: C,* vol. 111, p. 110862, 2020.

[3] B. Qiu, C. Zhao, J. Pan, Q. Zhou, and W. Yao, "Enhancing osteointegration and antibacterial properties of PEEK implants via AMP/HA dual-layer coatings," *Surfaces and Interfaces,* vol. 51, p. 104761, 2024.

[4] Z. Ma, X. Zhao, J. Zhao, Z. Zhao, Q. Wang, and C. Zhang, "Biologically modified polyether ether ketone as dental implant material," *Frontiers in Bioengineering and Biotechnology,* vol. 8, p. 620537, 2020.

[5] Y. Zheng *et al.*, "A programmed surface on polyetheretherketone for sequentially dictating osteoimmunomodulation and bone regeneration to achieve ameliorative osseointegration under osteoporotic conditions," *Bioactive materials,* vol. 14, pp. 364-376, 2022.

[6] M. A. Alsmael and A. Mohammed Al-Khafaji, "Improving surface properties of PEEK for dental applications by using piranha solution," *International Journal of Dentistry,* vol. 2023, no. 1, p. 7840601, 2023.

[7] A. S. Kadhum and A. F. Alhuwaizi, "The effect of composite bonding spot size and location on the performance of poly-ether-ether-ketone (PEEK) retainer wires," 2021.

[8] M. S. Tukmachi, H. J. Abdul-Baqi, and F. H. Hussein, "Biofunctionalization of polyetheretherketone implant material by bone-forming peptide-2 immobilization," *Karbala International Journal of Modern Science,* vol. 9, no. 1, p. 9, 2023.

[9] G. Pellegrini, L. Francetti, B. Barbaro, and M. Del Fabbro, "Novel surfaces and osseointegration in implant dentistry," *Journal of investigative and clinical dentistry,* vol. 9, no. 4, p. e12349, 2018.

[10] S. Gupta, S. Noumbissi, and M. F. Kunrath, "Nano modified zirconia dental implants: Advances and the frontiers for rapid osseointegration," *Medical Devices & Sensors,* vol. 3, no. 3, p. e10076, 2020.

[11] B. Chrcanovic, J. Kisch, T. Albrektsson, and A. Wennerberg, "Factors influencing early dental implant failures," *Journal of dental research,* vol. 95, no. 9, pp. 995-1002, 2016.

[12] Y. Yang *et al.*, "Toxicity assessment of nanoparticles in various systems and organs," *Nanotechnology Reviews,* vol. 6, no. 3, pp. 279-289, 2017.

[13] C. Gautam, J. Joyner, A. Gautam, J. Rao, and R. Vajtai, "Zirconia based dental ceramics: structure, mechanical properties, biocompatibility and applications," *Dalton transactions,* vol. 45, no. 48, pp. 19194-19215, 2016.

[14] M. M. Gad, A. Rahoma, A. M. Al-Thobity, and A. S. ArRejaie, "Influence of incorporation of ZrO2 nanoparticles on the repair strength of polymethyl methacrylate denture bases," *International journal of nanomedicine,* pp. 5633-5643, 2016.

[15] A. Velásquez and A. Arnedo, "Growth and characterization of magnetite-maghemite thin films by the dip coating method," *Hyperfine Interactions,* vol. 238, no. 1, p. 46, 2017.

[16] X. Tang and X. Yan, "Dip-coating for fibrous materials: mechanism, methods and applications," *Journal of Sol-Gel Science and Technology,* vol. 81, no. 2, pp. 378-404, 2017.

[17] R. Ma *et al.*, "Effects of different sulfonation times and post-treatment methods on the characterization and cytocompatibility of sulfonated PEEK," *Journal of biomaterials applications,* vol. 35, no. 3, pp. 342-352, 2020.

[18] P. Qiu, V. Bennani, P. Cooper, G. Dias, and J. Ratnayake, "Surface chemistry on PEEK surfaces: from enhanced biofunctionality to improved surface modifiability," *Applied materials today,* vol. 41, p. 102523, 2024.

[19] S. Luthfianto, E. Pujiyanto, C. N. Rosyidi, and P. W. Laksono, "Multi-Objective Optimization of the Dip-Coating Parameters for Polylactic Acid Plus Bone Screws Using Taguchi Method, Response Surface Methodology, and Non-Dominated Sorting Genetic Algorithm II," *Processes,* vol. 13, no. 6, p. 1690, 2025.

[20] H. Guo *et al.*, "Direct formation of amphiphilic crosslinked networks based on PVP as a marine anti-biofouling coating," *Chemical Engineering Journal,* vol. 374, pp. 1353-1363, 2019.

[21] C. Magdaleno-Lopez and J. de Jesus Perez-Bueno, "Quantitative evaluation for the ASTM D4541-17/D7234 and ASTM D3359 adhesion norms with digital optical microscopy for surface modifications with flame and APPJ," *International Journal of Adhesion and Adhesives,* vol. 98, p. 102551, 2020.

[22] C. Karunanithi, S. Natarajan, G. Manivasagam, and J. Sathiyanarayanan, "In vitro assessment of corrosion, antibacterial properties, and degradation behavior of zirconia-coated polyetheretherketone (PEEK)," *Journal of Bioactive and Compatible Polymers,* vol. 40, no. 1, pp. 45-67, 2025.

[23] T. Yabutsuka, K. Fukushima, T. Hiruta, S. Takai, and T. Yao, "Fabrication of bioactive fiber-reinforced PEEK and MXD6 by incorporation of precursor of apatite," *Journal of Biomedical Materials Research Part B: Applied Biomaterials,* vol. 106, no. 6, pp. 2254-2265, 2018.

[24] M. Topuz, "Effect of ZrO2 on morphological and adhesion properties of hydroxyapatite reinforced poly–(lactic) acid matrix hybrid coatings on Mg substrates," *Research on Engineering Structures and Materials,* vol. 8, pp. 721-733, 2022.

[25] C. Zhichun, L. Jianzhong, Z. Zhiying, Y. Wenhu, and Q. Donghai, "Effects of addition of polyvinyl pyrrolidone (PVP) as a corrosion inhibitor to Zr/V-based conversion coating on aluminum alloy," *Chemical Papers,* vol. 77, no. 10, pp. 5847-5857, 2023.

[26] T. Sopcak *et al.*, "Characterization and adhesion strength of porous electrosprayed polymer–hydroxyapatite composite coatings," *Resolution and Discovery,* vol. 3, no. 2, pp. 17-23, 2018.

[27] S. Tape, "Standard test methods for rating adhesion by tape Test1," ed, 2024.

[28] A. Grayeli *et al.*, "Thickness dependent crystallinity, hydrophilicity, and surface microtexture in CaF2 thin films deposited via thermal evaporation method," *Ceramics International,* vol. 51, no. 1, pp. 267-278, 2025.

[29] R. K. Jain, J. Kaur, A. Khanna, and A. K. Chawla, "Tailoring the structural, electrical, optical and wettability properties of ZnSe films by oblique angle thermal evaporation," *Materials Research Express,* vol. 6, no. 11, p. 116451, 2019.

[30] R. K. Jain, J. Kaur, S. Arora, A. Kumar, A. K. Chawla, and A. Khanna, "Effects of oblique angle deposition on structural, electrical and wettability properties of Bi thin films grown by thermal evaporation," *Applied Surface Science,* vol. 463, pp. 45-51, 2019.

[31] Y. Guo, Z. Wang, L. Zhang, X. Shen, and F. Liu, "Thickness dependence of surface energy and

contact angle of water droplets on ultrathin MoS 2 films," *Physical Chemistry Chemical Physics,* vol. 18, no. 21, pp. 14449-14453, 2016.

[32] G. R. M. Matos, "Surface roughness of dental implant and osseointegration," *Journal of maxillofacial and oral surgery,* vol. 20, no. 1, pp. 1-4, 2021.

[33] X. Wang *et al.*, "Tribological Performance and Enhancing Mechanism of 3D Printed PEEK Coated with In Situ ZIF-8 Nanomaterial," *Polymers,* vol. 16, no. 8, p. 1150, 2024.